



HAL
open science

An Analysis of Current and Electric Field Pulses Associated With Upward Negative Lightning Flashes Initiated from the Säntis Tower

Lixia He, Mohammad Azadifar, Farhad Rachidi, Marcos Rubinstein, Vladimir A Rakov, Vernon Cooray, Davide Pavanello, Hongyan Xing

► **To cite this version:**

Lixia He, Mohammad Azadifar, Farhad Rachidi, Marcos Rubinstein, Vladimir A Rakov, et al.. An Analysis of Current and Electric Field Pulses Associated With Upward Negative Lightning Flashes Initiated from the Säntis Tower. *Journal of Geophysical Research: Atmospheres*, 2018, 123 (8), pp.4045-4059. 10.1029/2018JD028295 . hal-01792255

HAL Id: hal-01792255

<https://ensta-paris.hal.science/hal-01792255>

Submitted on 27 Feb 2019

HAL is a multi-disciplinary open access archive for the deposit and dissemination of scientific research documents, whether they are published or not. The documents may come from teaching and research institutions in France or abroad, or from public or private research centers.

L'archive ouverte pluridisciplinaire **HAL**, est destinée au dépôt et à la diffusion de documents scientifiques de niveau recherche, publiés ou non, émanant des établissements d'enseignement et de recherche français ou étrangers, des laboratoires publics ou privés.

RESEARCH ARTICLE

10.1029/2018JD028295

Key Points:

- Four types of pulses are identified in current and associated 15-km electric field records of upward negative lightning flashes initiated from the Säntis Tower in Switzerland
- About 41% of mixed-mode ICC pulses were associated with microsecond-scale electric field pulses occurring some hundreds of microseconds prior to the onset of the current
- The characteristics of M-component-type pulses occurring during the initial stage (ICC pulses) are found to be similar to those of classical M components occurring during the continuing current after return strokes

Correspondence to:

F. Rachidi,
farhad.rachidi@epfl.ch

Citation:

He, L., Azadifar, M., Rachidi, F., Rubinstein, M., Rakov, V. A., Cooray, V., et al. (2018). An analysis of current and electric field pulses associated with upward negative lightning flashes initiated from the Säntis tower. *Journal of Geophysical Research: Atmospheres*, 123. <https://doi.org/10.1029/2018JD028295>

Received 8 JAN 2018

Accepted 28 MAR 2018

Accepted article online 9 APR 2018

An Analysis of Current and Electric Field Pulses Associated With Upward Negative Lightning Flashes Initiated from the Säntis Tower

Lixia He^{1,2} , Mohammad Azadifar^{2,3} , Farhad Rachidi² , Marcos Rubinstein³ , Vladimir A. Rakov^{4,5} , Vernon Cooray⁶, Davide Pavanello⁷ , and Hongyan Xing¹

¹Key Laboratory of Meteorological Disaster, Ministry of Education(KLME); Collaborative Innovation Center on Forecast and Evaluation of Meteorological Disasters (CIC-FEMD); Jiangsu Key Laboratory of Meteorological Observation and Information Processing, Nanjing University of Information Science and Technology, Nanjing, China, ²Electromagnetic Compatibility Laboratory, Swiss Federal Institute of Technology (EPFL), Lausanne, Switzerland, ³Institute of Information and Communication Technologies, University of Applied Sciences of Western Switzerland, Yverdon-les-Bains, Switzerland, ⁴Department of Electrical and Computer Engineering, University of Florida, Gainesville, FL, USA, ⁵Institute of Applied Physics, Russian Academy of Sciences, Nizhny Novgorod, Russia, ⁶Division for Electricity, Uppsala University, Uppsala, Sweden, ⁷The Institute of Systems Engineering, University of Applied Sciences of Western Switzerland, Sion, Switzerland

Abstract We present a study on the characteristics of current and electric field pulses associated with upward lightning flashes initiated from the instrumented Säntis Tower in Switzerland. The electric field was measured 15 km from the tower. Upward flashes always begin with the initial stage composed of the upward-leader phase and the initial-continuous-current (ICC) phase. Four types of current pulses are identified and analyzed in the paper: (1) return-stroke pulses, which occur after the extinction of the ICC and are preceded by essentially no-current time intervals; (2) mixed-mode ICC pulses, defined as fast pulses superimposed on the ICC, which have characteristics very similar to those of return strokes and are believed to be associated with the reactivation of a decayed branch or the connection of a newly created channel to the ICC-carrying channel at relatively small junction heights; (3) “classical” M-component pulses superimposed on the continuing current following some return strokes; and (4) M-component-type ICC pulses, presumably associated with the reactivation of a decayed branch or the connection of a newly created channel to the ICC-carrying channel at relatively large junction heights. We consider a data set consisting of 9 return-stroke pulses, 70 mixed-mode ICC pulses, 11 classical M-component pulses, and 19 M-component-type ICC pulses (a total of 109 pulses). The salient characteristics of the current and field waveforms are analyzed. A new criterion is proposed to distinguish between mixed-mode and M-component-type pulses, which is based on the current waveform features. The characteristics of M-component-type pulses during the initial stage are found to be similar to those of classical M-component pulses occurring during the continuing current after some return strokes. It is also found that about 41% of mixed-mode ICC pulses were preceded by microsecond-scale pulses occurring in electric field records some hundreds of microseconds prior to the onset of the current, very similar to microsecond-scale electric field pulses observed for M-component-type ICC pulses and which can be attributed to the junction of an in-cloud leader channel to the current-carrying channel to ground. Classical M-component pulses and M-component-type ICC pulses tend to have larger risetimes ranging from 6.3 to 430 μ s. On the other hand, return-stroke pulses and mixed-mode ICC pulses have current risetimes ranging from 0.5 to 28 μ s. Finally, our data suggest that the 8- μ s criterion for the current risetime proposed by Flache et al. is a reasonable tool to distinguish between return strokes and classical M-components. However, mixed-mode ICC pulses superimposed on the ICC can sometimes have considerably longer risetimes, up to about 28 μ s, as observed in this study.

1. Introduction

Characteristics and mechanisms of lightning flashes initiated from tall structures have been studied for nearly eight decades (e.g., Baba & Rakov, 2005; Berger, 1967; Bermudez et al., 2003; He et al., 2014; Heidler & Paul, 2017; McEachron, 1939; Miki et al., 2005; Mosaddeghi et al., 2011; Pavanello et al., 2007; Rachidi et al., 2001; Wang et al., 2008; Zhang et al., 2014; Zhou et al., 2012). The percentage of upward flashes initiated from

tall towers depends on a number of factors such as the height of the structure, the topographical conditions, and the presence of other tall structures in the vicinity (Smorgonskiy et al., 2013). For example, for the towers at Monte San Salvatore, upward flashes constitute about 70% (Berger, 1967), while for the Gaisberg and Sântis Towers, about 99% (Diendorfer et al., 2009) of the flashes are of upward type.

Lightning current waveforms associated with negative upward discharges begin with an initial-stage current, which consists of an upward positive leader current and a slowly varying current called the initial continuous current (ICC). After the extinction of the ICC, one or more downward-leader/upward-return-stroke sequences can occur (Rakov & Uman, 2003). A significant fraction of upward negative lightning flashes (for example, 52% for the Gaisberg tower; Diendorfer et al., 2009) are characterized by the presence of pulses superimposed on the ICC, the so-called ICC pulses.

Zhou et al. (2015) have associated ICC pulses with either (i) M-component mode of charge transfer to ground, typically along a single channel below the cloud base, which implies a relatively large distance between the excitation (junction) point and the tower top, or (ii) downward leader/return-stroke processes, in a decayed branch or a newly created channel connected to the ICC-carrying channel at relatively short distance from the tower top. The term “mixed mode of charge transfer to ground” was proposed by Zhou et al. (2011) to describe this latter case, as opposed to the “classical” M-component mode, which is characterized by a relatively high junction point (see Figure 15 of Zhou et al., 2015).

Significant differences exist between the mechanisms of charge transfer to ground in leader/return-stroke sequences and in M components, associated with 5 to 6 orders of magnitude difference in conductivity of the available path to ground (Rakov et al., 2001). Return-stroke peak currents range from a few kiloamperes to a few hundred kiloamperes with risetimes (RTs) usually not exceeding several microseconds and being much shorter than fall time. A typical M component is characterized by a more or less symmetrical channel-base current waveform with a much lower peak and considerably longer RT compared to those associated with a typical return stroke (Fisher et al., 1993; Thottappillil et al., 1995). The associated close electric field signature is characterized by a millisecond-scale hook shape and microsecond-scale pulses (Rakov et al., 1992) prior to the onset of the current, which were inferred to be associated with the contact between an in-cloud leader and the current-carrying channel to ground (Rakov et al., 2001). Analyzing high-speed video images and current records of upward flashes observed at the Peissenberg Tower in Germany, Flache et al. (2008) found that ICC pulses with RTs of about 8 μ s or greater tended to be associated with the M-component mode of charge transfer to ground, while those with RTs shorter than about 8 μ s tended to be associated with the leader/return-stroke mode.

One of the features of M components distinguishing them from leader/return-stroke sequences is the fact that the peak of close electric field signature lags the onset of channel-base current (Rakov et al., 1995). Based on the observations of rocket-triggered lightning flashes in China, Qie et al. (2011) found that the time interval between the current onset and the close electric field peak for M-component pulses or M-component-type ICC pulses was some tens of microseconds, while for leader/return-stroke sequences, this time interval was less than 1 μ s. Zhou et al. (2015) found that the value for this time interval equal to 10 μ s could be used as a criterion to distinguish between mixed-mode ICC and M-component-type pulses. Making use of the simultaneous current and electric field data obtained at the instrumented Sântis Tower in Switzerland and associated electromagnetic field measuring system, Azadifar et al. (2016) studied the characteristics of fast pulses superimposed on the initial continuous current in upward negative lightning flashes. They found that their characteristics are very similar to those of return strokes, suggesting that these pulses are indeed associated with the mixed-mode charge transfer to ground.

In this paper, we analyze the salient characteristics of pulses in upward negative flashes. The study is based on simultaneous records of current and corresponding electric fields at 15 km associated with upward flashes initiated from the Sântis Tower.

The rest of the paper is organized as follows. Section 2 briefly describes the current measurement system at the Sântis Tower and the electric field measuring system in Herisau, located about 15 km (14.7 km) from the tower. Section 3 includes an overall presentation of the data set and the classification of the pulses. Section 4 presents the definitions of the parameters in this study, as well as the characteristics and comparison of the four types of pulses. Finally, a summary and conclusions are given in section 5.

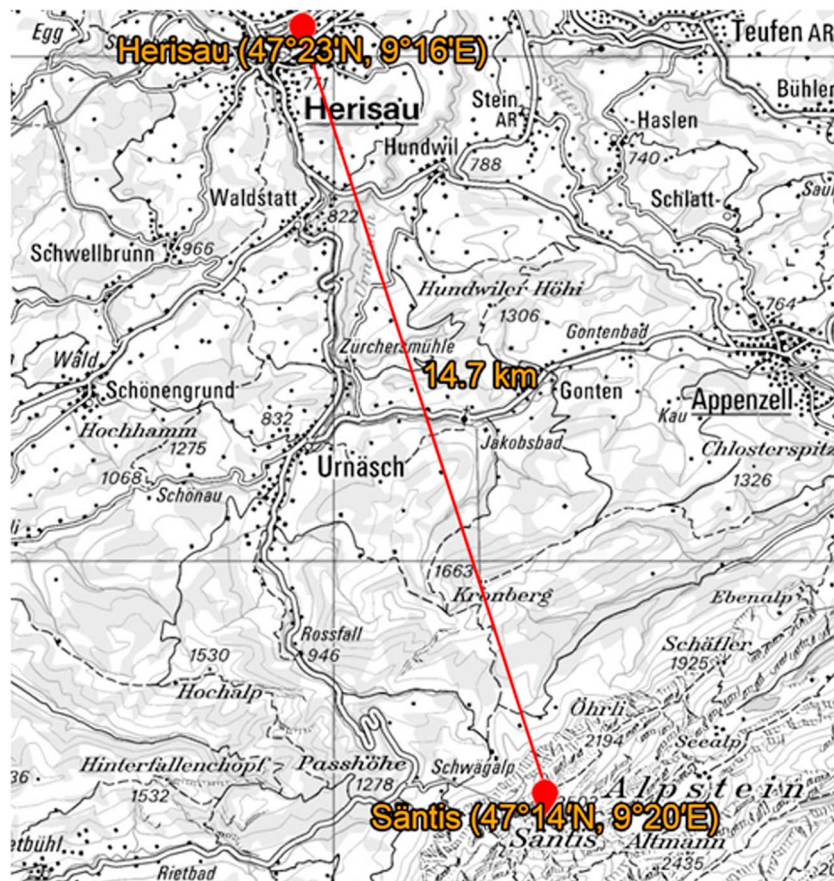


Figure 1. Locations of the Sântis Tower and the field measuring station in Herisau.

It is worth noting that throughout the paper, (i) a positive sign for the current is used for negative return strokes and (ii) the atmospheric electricity sign convention (downward directed electric field or electric field change vector is positive) is adopted for the electric field.

2. Experimental Setup

The lightning current measuring system at the Sântis Tower in Switzerland was deployed in May 2010. The lightning current and the current derivative are measured using Rogowski coils and multigap B-Dot sensors mounted at two heights, 24 and 82 m, along the tower (Azadifar et al., 2014; Romero et al., 2010). The electric field measuring system was located 14.7 km away from the Sântis Tower and comprised a flat-plate antenna and an analog integrator with an overall frequency bandwidth of 30 Hz to 2 MHz. The output signal of the integrator was transferred to an industrial PC using LTX5515 E/O and O/E convertors and a 100-m long fiber optic cable. The signal was digitized and recorded using a PCI 5122 National Instruments card with sampling rate of 5 MS/s and a record length of 4 s. The field sensor was installed on the roof of a 25-m tall building in Herisau (Li et al., 2016). Locations of the Sântis Tower and the field measuring station in Herisau are shown in Figure 1. The electric field sensor was calibrated in the high-voltage laboratory of the Swiss Federal Institute of Technology. It is worth noting that enhancement effects on the electric field due to the presence of the building and also propagation effect along a mountainous terrain (see e.g., Li et al., 2016) were not considered in this work.

3. Data and Methodology

3.1. Data

The analyzed data set consists of three upward negative flashes recorded in August 2016, which contained a total of 109 pulses (including ICC pulses, classical M-component pulses, and return strokes). It is worth noting

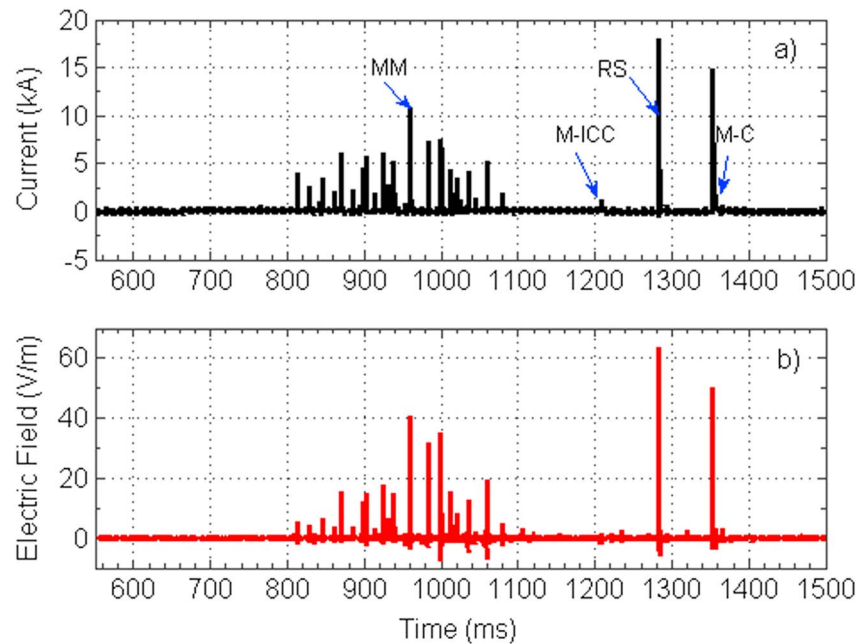


Figure 2. (a) Overall current waveform and (b) simultaneous E-field waveform at about 15 km of a flash that occurred on 4 August 2016 at 23:57. Examples of four types of pulses are labeled in Figure 2a; they are shown on expanded time scales in Figures 4, 5, and 7–9.

that GPS time stamps were not available for the considered events and the current and field data were time correlated by analyzing the interpulse interval pattern. The field and current waveforms were aligned following the same procedure as in Azadifar et al. (2016), using the last return stroke of each flash, which can provide sufficiently accurate alignment with an error of the order of a few microseconds.

The 109 pulses during the three flashes are classified into four types depending on the expected mechanism of charge transfer to ground (see section 1):

1. Return-stroke pulses (RS): Pulses that appear after the extinction of the ICC and are preceded by an essentially no-current interval.
2. Mixed-mode ICC pulses (MM): Fast asymmetrical (fast-RT) pulses superimposed on the ICC. These pulses are believed to be associated with the reactivation of a decayed branch or the connection of a newly created channel to the ICC-carrying channel to ground at low junction points (Zhou et al., 2015).
3. Classical M-component pulses (M-C): Pulses superimposed on the continuing current that follows some return strokes (Rakov et al., 1995).
4. M-component-type ICC pulses (M-ICC): Pulses superimposed on the ICC and characterized by a more or less symmetrical (slow-RT) waveform. These pulses are believed to be associated with the reactivation of a decayed branch or the connection of a newly created channel to the ICC-carrying channel to ground at high junction points (Zhou et al., 2015).

Each of the 109 pulses in the considered data set was assigned to one of the four above-mentioned categories. The sample sizes of those categories were as follows:

1. 9 return-stroke pulses (RS);
2. 70 mixed-mode ICC pulses (MM);
3. 11 classical M-component pulses (M-C); and
4. 19 M-component-type ICC pulses (M-ICC).

Figure 2 presents the channel-base current and electric field waveforms at about 15 km associated with a flash that occurred on 4 August 2016 at 23:57. The initial stage of this flash lasted for about 600 ms and was followed by two return strokes. This flash contained all four types of pulses described above, examples of which will be presented below.

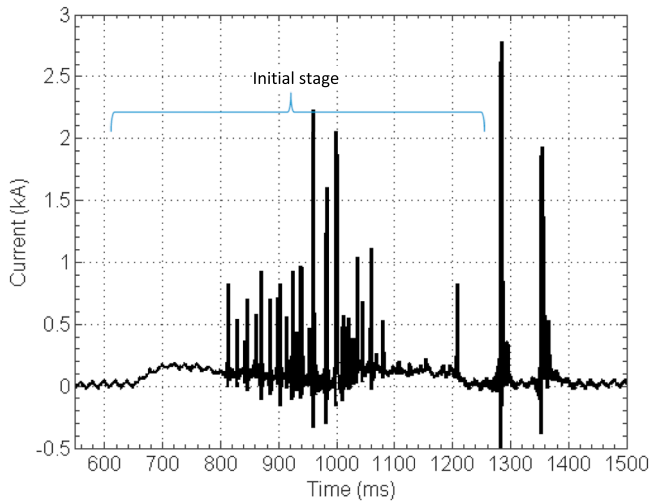


Figure 3. Current waveform shown in Figure 2 after filtering with 1 kHz low-pass filter to accentuate the slowly varying initial-stage current.

Figure 3 shows the current waveform to which a low-pass zero-phase filter with a cutoff frequency of 1 kHz was applied. In this figure, the initial stage, which starts at about 650 ms and lasts until about 1,220 ms, can be clearly identified.

Current and field waveforms associated with each of the four types of pulses (marked in Figure 2a) will be presented below.

3.1.1. Return-Stroke Pulses (RS)

Figure 4 presents an expanded view of the current and field waveforms associated with one of the two return strokes (labeled RS in Figure 2a) of the flash shown in Figure 2. The current is characterized by a peak value of 18.4 kA, a 10-to-90% risetime (henceforth called RT) of 1.6 μ s, and a duration (full width at half maximum, FWHM) of 40.3 μ s. The electric field has a peak value of 69.7 V/m, an RT of 1.4 μ s, and a duration (FWHM) of 2.8 μ s.

3.1.2. Mixed-Mode ICC Pulses (MM)

Figure 5 presents an expanded view of the current and field waveforms associated with a mixed-mode ICC pulse (labeled MM in Figure 2a) of the same flash (the total number of the mixed-mode pulses in this flash is 25). The current is characterized by a peak value of 10.8 kA, an RT of

2.7 μ s, and a duration (FWHM) of 58 μ s. The associated electric field has a peak value of 44.3 V/m, an RT of 1.6 μ s, and a duration (FWHM) of 3.2 μ s. As discussed in Azadifar et al. (2016), the characteristics of these pulses are very similar to those of return strokes.

About 41% of mixed-mode ICC pulses were preceded by fast (microsecond-scale) electric field pulses occurring some hundreds of microseconds prior to the onset of the current, very similar to those observed for M-component-type ICC pulses. As an example, Figure 6 shows a set of current and field waveforms associated with the mixed mode of charge transfer to ground, in which fast pulses occurring 150 and 300 μ s prior to the onset of currents can be seen. In this example, the current is characterized by a peak value of 2.3 kA, an RT of 19 μ s, and a duration (FWHM) of 40.4 μ s. The corresponding electric field has a peak value of 4 V/m, an RT of 7.6 μ s, and a duration (FWHM) of 3.8 μ s. Note that another, smaller M-component-type ICC pulse is seen in both the current and the field waveforms at a time of about 909.4 ms. The latter is not further discussed in this paper.

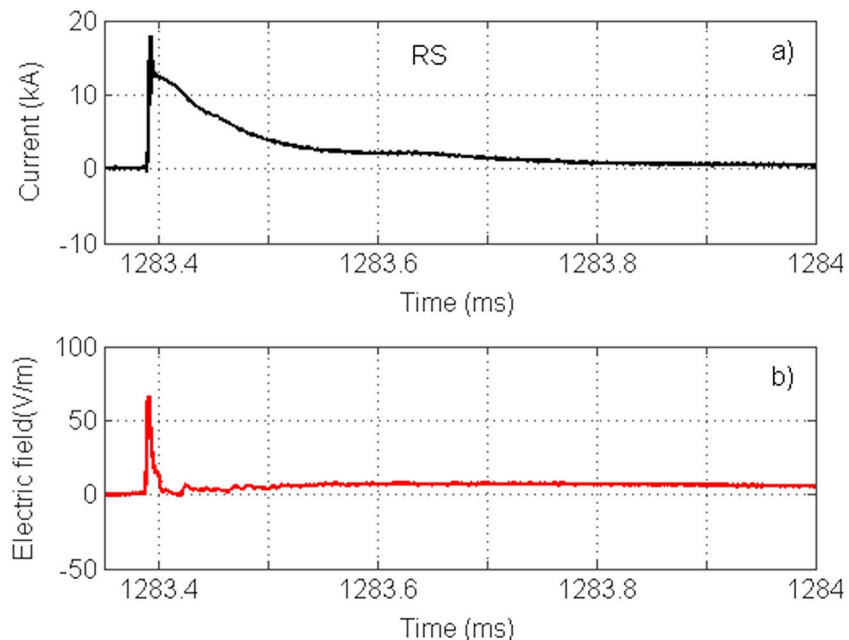


Figure 4. Expanded views of (a) the current and (b) the simultaneous E-field waveforms of the return stroke of the flash whose overall records are presented in Figure 2 (see pulse labeled RS).

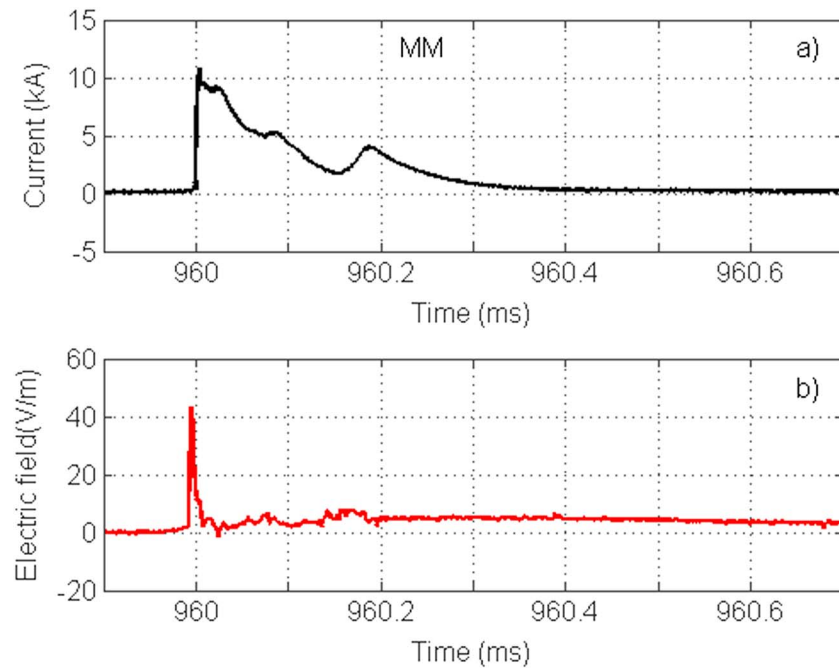


Figure 5. Expanded views of (a) the current and (b) the simultaneous E-field waveforms of a mixed-mode ICC pulse of the flash whose overall records are presented in Figure 2 (see pulse labeled MM). Junction-process electric field pulses are not seen in Figure 5b and are illustrated (for a different mixed-mode ICC pulse) in Figure 6b.

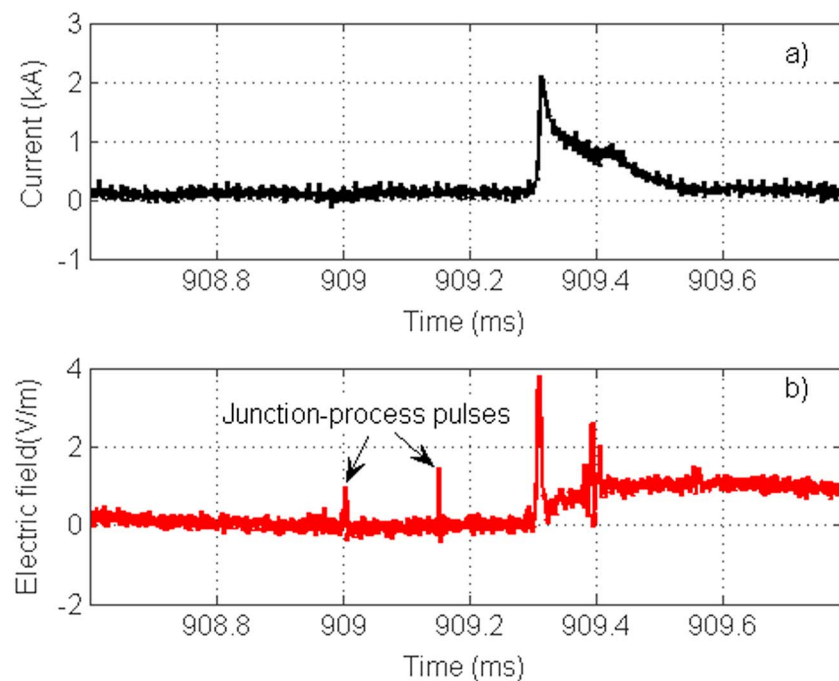


Figure 6. Expanded views of (a) the current and (b) the simultaneous E-field waveforms of a mixed-mode ICC pulse featuring junction-process E-field pulses prior to the onset of the current, which are similar to those associated with M-component-type ICC pulses. This event belongs to the flash that occurred on 10 August 2016 at 17:39.

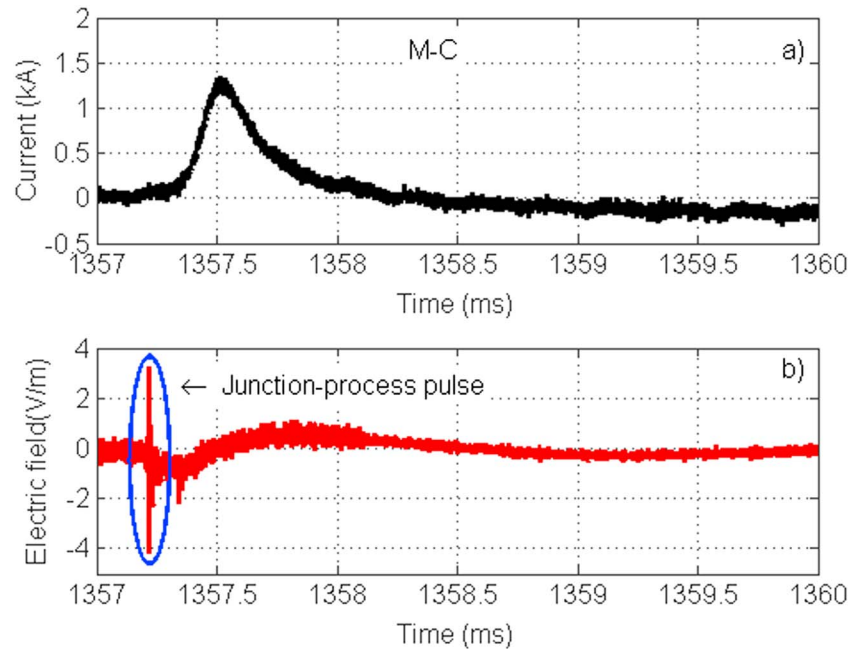


Figure 7. Expanded views of (a) the current and (b) the simultaneous E-field waveforms of a classical M-component pulse in the flash whose overall records are presented in Figure 2 (see pulse labeled M-C). The microsecond-scale bipolar electric field pulse apparently associated with the junction process in the cloud is marked by a blue ellipse.

3.1.3. Classical M-Component Pulses (M-C)

Figure 7 presents an expanded view of the current and field waveforms associated with an M-component (labeled M-C in Figure 2a) in the same flash. As one can see, the current is characterized by a much slower waveform compared to return-stroke pulses and mixed-mode ICC pulses. The 15-km electric field waveform shown in Figure 7b and corresponding to the current waveform seen in Figure 7a is unpronounced. It is preceded by a microsecond-scale bipolar pulse (see Figure 8) occurring about 150 μ s prior to the onset of the current pulse. Following Pichler et al. (2010), Rakov et al. (2001), and Tran et al. (2013), we attribute the microsecond-scale pulse to the junction of an in-cloud leader channel to the current-carrying channel to ground.

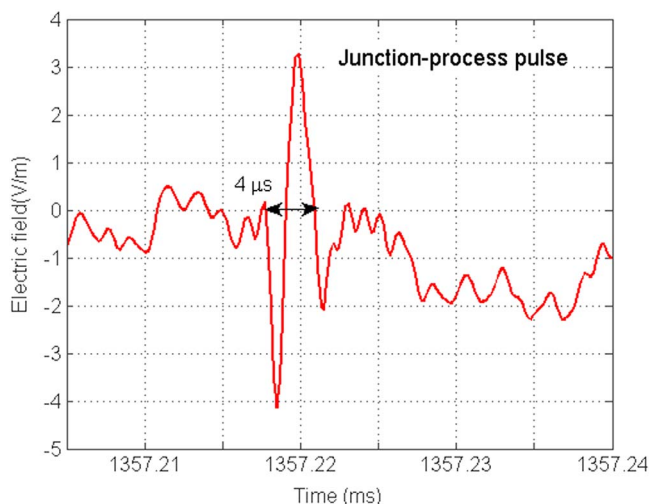


Figure 8. Expanded view of the microsecond-scale bipolar electric field pulse shown (enclosed by a blue ellipse) in Figure 7.

The hook-shaped electric field waveform that is characteristic of M components is usually observed at distances not exceeding a few kilometers (Rakov et al., 1992). The slow part of the field waveform shown in Figure 7b is unpronounced because of the relatively large distance of 15 km. It is apparently dominated by electrostatic and induction components, as opposed to the microsecond scale (see Figure 8), which is essentially radiation component. The full width of the junction-process pulse shown in Figure 8 is about 4 μ s, the initial negative half-cycle magnitude is -4 V/m, and the positive half-cycle magnitude is $+3.2$ V/m.

3.1.4. M-Component-Type ICC Pulses (M-ICC)

Figure 9 presents an expanded view of the current and field waveforms associated with an M-component-type ICC pulse (labeled M-ICC in Figure 2a) in the same flash. It is clear that the characteristics of the current and field waveforms are very similar to those of classical M-components (compare Figures 7 and 9).

3.2. Pulse Classification Method

The criteria for the classification of the observed return-stroke and M-component pulses are quite straightforward. Return strokes occur after the extinction of the initial continuous currents and are preceded by

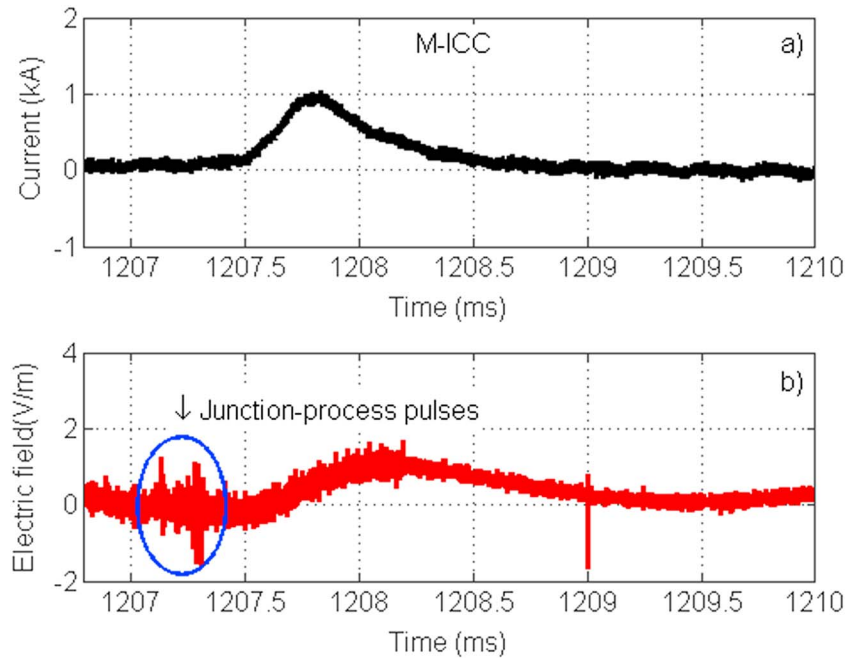


Figure 9. Expanded views of (a) the current and (b) the simultaneous E-field waveforms of an M-component-type ICC pulse in the flash whose overall records are presented in Figure 2 (see pulse labeled M-ICC).

an essentially no-current interval, while M components occur during the continuing current that follows some return strokes. On the other hand, the distinction between M-component-type ICC pulses and mixed-mode ICC pulses is not always clear. Zhou et al. (2015) used the time interval between the current onset and the close (170 m) electric field peak to distinguish mixed-mode ICC pulses from M-component-type ICC pulses. In this study, it was not possible to use this criterion because our electric fields were measured about 15 km from the tower. At such a large distance, M-component-type processes usually do not produce the V-shaped close electric field signatures used by Zhou et al. (2015)

The criterion used in this study to distinguish between the mixed-mode ICC pulses and M-component-type ICC pulses was essentially based on the current waveform signature. As discussed in Rakov et al. (1995) and Rakov et al. (2001), the current associated with the M-component mode of charge transfer to ground has a more or less symmetrical waveform, while mixed-mode ICC pulses are characterized by current waveforms typical of return strokes (Azadifar et al., 2016). This feature was used to distinguish between these two types of pulses. Specifically, we used the asymmetrical waveform coefficient (AsWC) to quantify the asymmetry of each current pulse:

$$AsWC = \frac{FWHM - t_{50\%-100\%}}{FWHM} \quad (1)$$

where $t_{50\%-100\%}$ represents the time interval during which the current rises from 50% to 100% of its peak value. The calculation of AsWC is illustrated in Figure 10.

A fully symmetrical pulse is characterized by an AsWC equal to 1/2, while waveform characteristics of return strokes have AsWCs close to 1.0. Figure 11 presents the distribution (in terms of the number of pulses) of AsWC for the four types of pulses, (a) for return-stroke pulses (in grey) and classical M-component pulses (in red) and (b) for mixed-mode ICC pulses (in blue) and M-component-type ICC pulses (in green). As seen in Figure 11a, AsWC for return strokes ranges from 0.95 to 0.99, while for

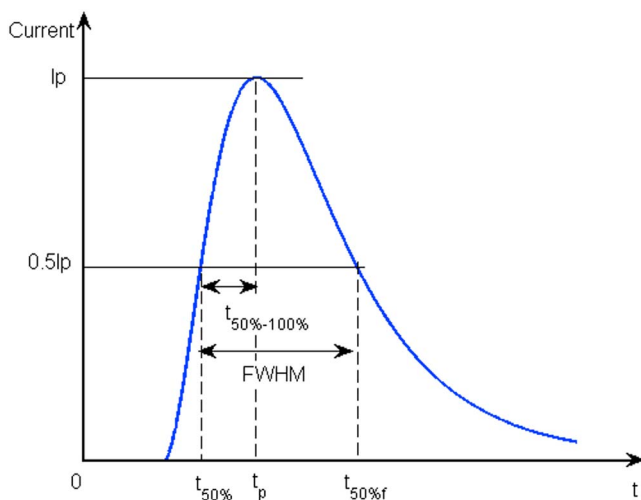


Figure 10. Definitions of parameters (FWHM and $t_{50\%-100\%}$) needed for calculation of the asymmetrical waveform coefficient (AsWC), using equation (1).

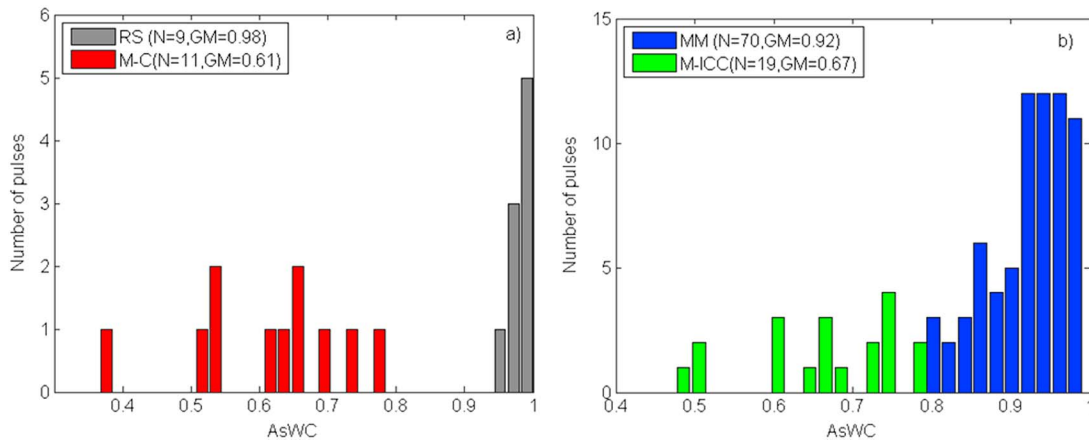


Figure 11. Distributions of AsWC for (a) return-stroke pulses and classical M-component pulses and (b) mixed-mode ICC pulses and M-component-type ICC pulses.

classical M-component pulses, it ranges from 0.38 to 0.78; that is, there is a clear separation in the ranges of AsWC for return strokes and M components. Considering on the one hand the clear difference in the AsWC ranges for return strokes and M components and, on the other hand, the similarity between (i) mixed-mode ICC pulses and return-stroke pulses and (ii) M-component-type ICC pulses and classical M-components, we have chosen a value $AsWC = 0.8$ as a criterion to distinguish M-component-type ICC pulses and mixed-mode ICC pulses. Specifically, if AsWC for a pulse superimposed on the ICC is lower than 0.8, the pulse is classified as an M-component-type ICC pulse. Otherwise, it is classified as a mixed-mode ICC pulse. Examining Figure 11b, one can see that AsWC values for mixed-mode ICC pulses range from 0.80 to 0.996, while for M-component-type ICC pulses, they range from 0.49 to 0.79, with no clear gap between the two ranges, in contrast with the case of return strokes and M components. This can be explained by the fact that the main difference between the mixed-mode ICC pulses and M-component-type ICC pulses is their junction point height, namely, less than 1 km or so for mixed-mode ICC pulses and greater than 1 km or so for M-component-type ICC pulses, according to the observations presented in Zhou et al. (2015). Significant uncertainty in junction point heights for these two types of pulses does not allow one to clearly define a demarcation line between mixed-mode ICC pulses and M-component-type ICC pulses in terms of the AsWC.

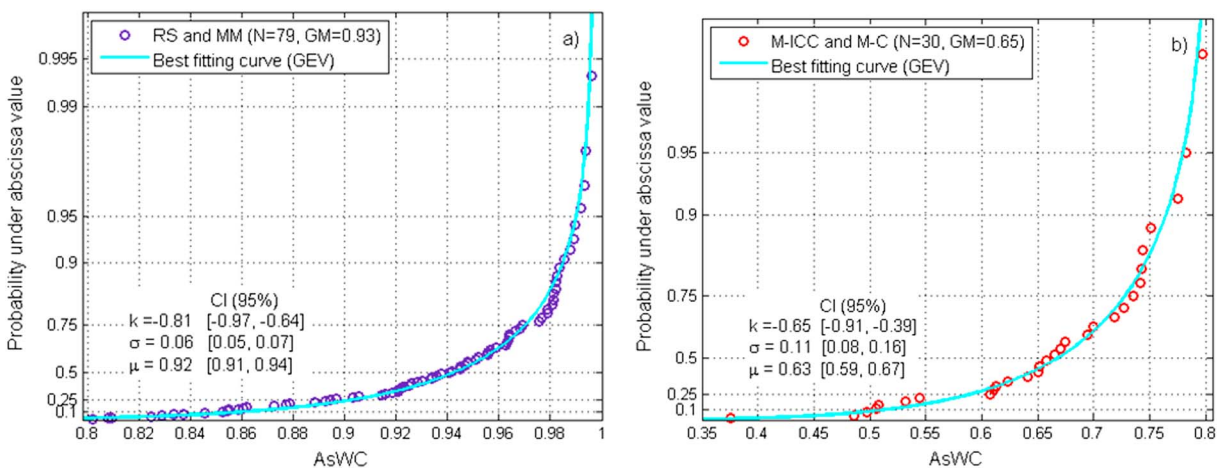


Figure 12. Cumulative probability distributions of AsWC for (a) RS and MM pulses combined and (b) M-ICC and M-C pulses combined. The distribution of AsWC follows the generally extreme value (GEV) distribution with three parameters: shape parameter (k), scale parameter (σ) and location parameter (μ). These parameters are different for RS and MM pulses combined (see Figure 12a) and M-ICC and M-C pulses combined (see Figure 12b). The associated 95% confidence interval (CI) is given for each parameter.

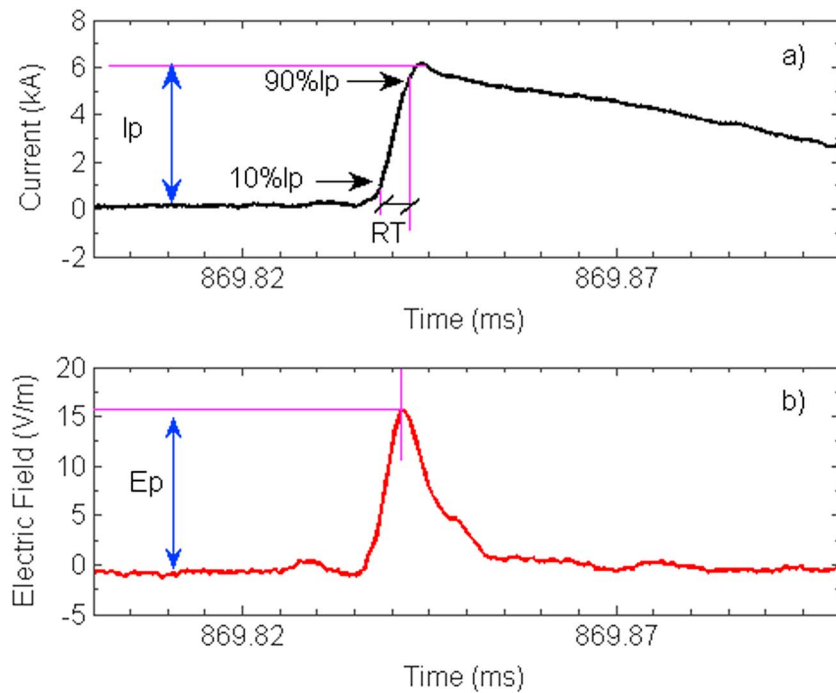


Figure 13. Definitions of parameters for return-stroke pulses and mixed-mode ICC pulses. (a) Current pulse and (b) E-field pulse at 15 km.

Figure 12a presents the cumulative probability distribution of AsWC for all the 30 classical M-component pulses and M-component-type ICC pulses combined. A similar distribution for all the 79 return-stroke pulses and mixed-mode ICC pulses combined is shown in Figure 12b. It can be seen that AsWC in both cases follows the generalized extreme value distribution (Coles et al., 2001) with different fitting curve parameters (k , σ ,

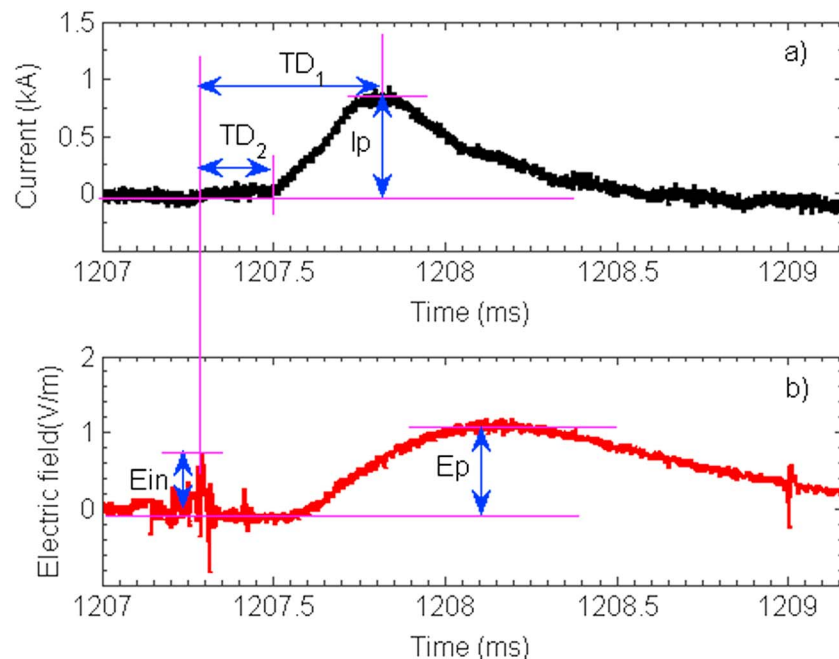


Figure 14. Definitions of parameters for M-component-type ICC pulses (M-ICC) and classical M-component pulses. (a) Current pulse and (b) E-field pulse at 15 km.

Table 1
Characteristics of Current and Electric Field Waveforms for Four Types of Pulses (Median and AM Values)

Pulse type	N	RT/ μ s		I_p /kA		E_p /(V/m)		E_p/I_p /(V/m/kA)		FWHM/ μ s		AsWC		TD1/ μ s		$ E_{in} $ /(V/m)		TD2/ μ s	
		M	AM	M	AM	M	AM	M	AM	M	AM	M	AM	M	AM	M	AM	M	AM
M-ICC	19	83.1	119.4	1.5	2.0	2.5	4.8	1.9	2.0	109.0	140.2	0.67	0.67	266.4	348.3	1.8	2.6	168.6	222.6
M-C	11	186.5	177.3	1.8	2.4	2.0	3.5	1.2	1.4	240.0	225.7	0.64	0.61	268.2	393.0	1.5	1.6	120.7	233.1
MM	70	4.4	5.5	4.0	4.9	14.7	17.6	3.5	3.2	49.2	57.3	0.83	0.92	129.0 ^a	206.5 ^a	2.0 ^a	2.1 ^a	98.4 ^a	221.1 ^a
RS	9	0.7	0.9	9.2	10.0	41.2	40.1	3.8	4.0	31.4	37.3	0.98	0.98	---	---	---	---	---	---

Note. M: median value; AM: arithmetic mean value.

^aThese values correspond to 34 out of 70 mixed-mode ICC pulses, which exhibited the junction-process microsecond-scale electric field pulses before the onset of the current.

and μ), which are given in Figures 12a and 12b, respectively. Parameters k , σ , and μ are, respectively, the shape parameter, the scale parameter, and the location parameter. The shape parameter k is negative in both cases, corresponding to the Type-III generalized extreme value distribution (belonging to the Weibull family) with an upper end point $-\sigma/k + \mu$ (0.9965 for return-stroke pulses and 0.8047 for M-component pulses).

The arithmetic mean value of AsWC for classical M-component pulses and M-component-type ICC pulses combined is about 0.65, while the arithmetic mean value of AsWC for return-stroke pulses and mixed-mode ICC pulses combined is 0.93.

4. Analysis and Discussion

4.1. Definition of the Parameters

The parameters used in this paper to characterize the four types of pulses are defined in Figure 13 (for return-stroke pulses and mixed-mode ICC pulses) and in Figure 14 (for classical M-component pulses and M-component-type ICC pulses).

In these figures, I_p represents the peak current and E_p represents the global peak of the corresponding electric field signature (excluding the junction-process microsecond-scale pulses, if any). In Figure 14, E_{in} is the largest peak of the junction-process E-field pulse or pulses. TD₁ is the time interval between the largest junction-process E-field pulse peak in Figure 14b and the current peak in Figure 14a, and TD₂ is the time interval between the largest junction-process E-field pulse peak and the onset of the current waveform.

In addition to the above parameters, we also measured the current RT, defined as the time interval between 10% and 90% of the pulse peak value at the current wavefront, as shown in Figure 13a.

4.2. Data Analysis and Comparison of Different Types of Pulses

Table 1 presents the arithmetic mean (AM) and median values (M) of the parameters of the current and electric field waveforms for each pulse type. Table 2 presents the ranges of the variation of the considered parameters.

The shortest observed RT for classical M-component pulses was 18.5 μ s, and 6.3 μ s for M-component-type ICC pulses, while the RTs for return-stroke pulses range from 0.6 to 1.9 μ s, and the RTs for mixed-mode ICC pulses range from 0.5 to 27.6 μ s.

The characteristics of M-component-type ICC pulses are generally similar to those of classical M-component pulses occurring during the continuing current following return strokes. The time intervals between the largest junction-process field pulse and the current (TD₁ for the current peak and TD₂ for the current onset, respectively) for classical M-components are on average longer than for M-component-type ICC pulses. This might indicate that the heights of the junction points for M-component-type ICC pulses are on average lower than for classical M-component pulses.

Figure 15 presents scatter plots of the electric field peak versus current peak for M-component-type ICC pulses and classical M-component pulses (Figure 15a), and for return-stroke pulses and mixed-mode ICC pulses (Figure 15b).

The sample sizes for pulses presented in Figure 15a are rather small to draw definitive conclusions. However, it can be seen that classical M-component (M-C) pulses are characterized by smaller peak field to peak current ratios compared to M-component-type ICC (M-ICC) pulses.

Table 2
The Minima and Maxima of the Waveform Parameters Listed in Table 1

Pulse type	RT/ μ s	I_p /kA	E_p /(V/m)	E_p/I_p /(V/m/kA)	FWHM/ μ s	AsWC	TD1/ μ s	$ E_{in} $ /(V/m)	TD2/ μ s
M-ICC	6.3–400.6	0.9–7.1	1.0–35.2	0.9–5.0	28.3–378.5	0.486–0.798	58.5–1064.0	0.4–15.0	7.2–761.1
M-C	18.5–429.8	0.6–7.4	1.0–17.1	0.7–2.3	31.7–368.7	0.376–0.776	38.8–1340.3	0.6–3.8	2.8–941.6
MM	0.5–27.6	1.0–18.0	1.6–79.7	1.2–4.9	8.6–197.7	0.802–0.996	22.1–1026.0 ^a	0.7–5.0 ^a	18.2–1019.0 ^a
RS	0.6–1.9	2.3–18.4	7.8–67.7	3.4–4.6	21.4–61.3	0.952–0.994	---	---	---

^aThese values correspond to 34 out of 70 mixed-mode ICC pulses, which exhibited the junction-process microsecond-scale electric field pulses before the onset of the current.

In agreement with the analysis presented in Zhou et al. (2015) and Azadifar et al. (2016), it is seen in Figure 15b that the peak field to peak current ratios for mixed-mode ICC pulses are very similar to those for return-stroke pulses. On the other hand, mixed-mode ICC pulses have generally smaller current and field peaks compared to return-stroke pulses (compare the corresponding median and AM values in Table 1). Specifically, 94% (66 of 70) of the mixed-mode ICC pulses have a peak current smaller than 10 kA, while only 56% (5 of 9) of return-stroke pulses do so.

Figure 16 shows histograms of the current pulse RTs. One can see that M-component (M-ICC and M-C) pulses are characterized by RTs ranging from 6.3 to 430 μ s, while return-stroke and mixed-mode ICC pulses have current RTs ranging from 0.6 to 27.6 μ s.

As mentioned in section 1, Flache et al. (2008), who analyzed high-speed video images and corresponding current records of upward discharges initiated by the Peissenberg Tower in Germany, found that ICC pulses with RTs of about 8 μ s (corresponding to the dotted cyan line shown in Figure 16) or greater tended to be associated with the M-component mode of charge transfer to ground, while those with RTs shorter than about 8 μ s tended to be associated with the return-stroke mode of charge transfer to ground. This criterion was used in some studies (e.g., Romero et al., 2013) to distinguish between return-stroke/mixed-mode ICC pulses and M-component pulses. As expected, all the return strokes in the present study are characterized

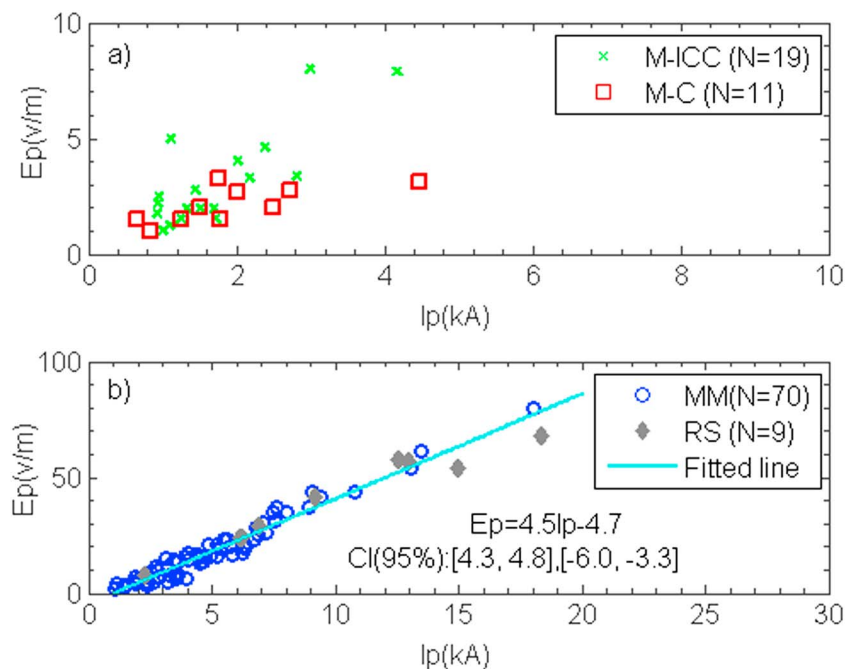


Figure 15. Scatter plots of the electric field peak versus current peak for (a) M-ICC pulses (green crosses) and M-C pulses (red squares) and (b) RS pulses (grey diamond) and MM pulses (blue circles). In (b), the regression line is expressed as $E_p = 4.5I_p - 4.7$, with 95% confidence intervals of [4.3, 4.8] and [-6.0, 3.3] for E_p and I_p , respectively.

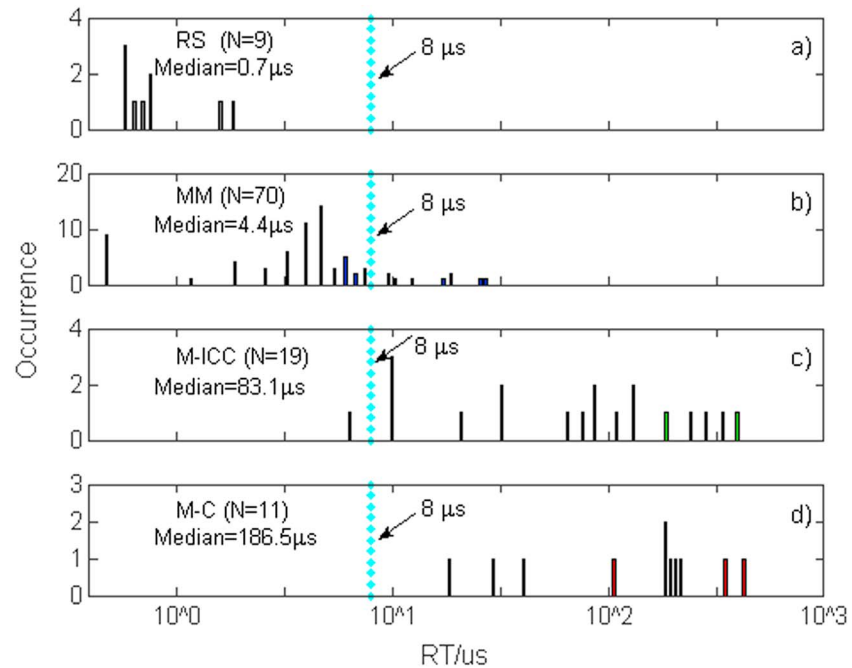


Figure 16. Histograms of current risetime for four types of pulses.

by RTs smaller than 8 μs , which is in line with previous studies, and all the classical M-component pulses have RTs larger than 8 μs . However, about 12.9% (9 of 70) of mixed-mode ICC pulses have RTs in excess of 8 μs and about 23.3% (7 of 30) of M-component-type ICC pulses have a RT smaller than 27.6 μs .

The data presented in Figure 16 suggest that the 8- μs threshold found by Flache et al. (2008) can be used to distinguish between return strokes and M-components (M-C). However, mixed-mode ICC pulses that are usually assumed to be manifestations of the leader/return-stroke mode of charge transfer to ground can sometimes have RTs longer than 8 μs , up to 27.6 μs as observed in this study.

5. Summary and Conclusions

We presented a study on the characteristics of current and electric field pulses associated with upward lightning flashes initiated from the Säntis Tower in Switzerland. The electric field was measured at a distance of 15 km from the tower.

Four types of current pulses were identified and analyzed in the paper: (1) return-stroke pulses, which occur after the extinction of the initial continuous current (ICC) and are preceded by an essentially no-current interval; (2) mixed-mode ICC pulses, which have characteristics very similar to those of return strokes and are believed to be associated with the reactivation of a decayed branch or the connection of a newly created channel to the ICC-carrying channel at low junction points; (3) classical M-component pulses superimposed on the continuing current following some return strokes; and (4) M-component-type ICC pulses, presumably associated with the reactivation of a decayed branch or the connection of a newly created channel to the ICC-carrying channel at high junction points.

We considered a data set comprising 109 pulses, including 9 return-stroke pulses, 70 mixed-mode ICC pulses, 11 classical M-component pulses, and 19 M-component-type ICC pulses. The salient characteristics of the current and corresponding electric field waveforms were analyzed. A new approach based on the degree of symmetry of the current waveform was proposed to distinguish between mixed-mode and M-component-type ICC pulses.

The characteristics of M-component-type ICC pulses were found to be similar to those of classical M-component pulses occurring during the post-return-stroke continuing current. It was also found that about 41% of mixed-mode ICC pulses were preceded by microsecond-scale electric field pulses occurring some

hundreds of microseconds prior to the onset of the current and apparently corresponding to the junction process. Interestingly, the median value of TD_1 for mixed-mode ICC pulses is about a factor of 2 smaller than for either classical M-component pulses or M-component-type ICC pulses, possibly suggesting a higher typical junction point for the latter two types of pulses. M-component-type ICC pulses combined with classical M-component pulses are characterized by RTs ranging from 6.3 to 430 μs , while return-stroke pulses and mixed-mode ICC pulses have current RTs ranging from 0.5 to 28 μs . Finally, our data suggest that the 8- μs threshold for the current RT proposed by Flache et al. (2008) can be used to distinguish between return strokes and classical M-components. However, mixed-mode ICC pulses can sometimes have RTs longer than 8 μs , up to about 28 μs as observed in this study, and M-component-type ICC pulses can occasionally have RTs shorter than 8 μs . Additional data are needed to make more statistically reliable conclusions.

Acknowledgments

Financial supports from the following funding agencies are acknowledged: Swiss National Science Foundation (project 200021_147058), European Union's Horizon 2020 research and innovation program (grant agreement 737033-LLR), the Research Innovation Program of Colleges and Universities Postgraduates of Jiangsu Province, China (grant KYZZ15_0245), and China Scholarship Council (CSC). The work was also supported in part by NSF grant AGS-1701484, the National Natural Science Foundation of China (grant 61671248), Major Projects of Natural Science Research in Universities of Jiangsu Province (15KJA460008), and The Priority Academic Program Development of Jiangsu Higher Education Institutions (PAPD). All the lightning current data presented in this paper are available from Zenodo repository (doi:10.5281/zenodo.1208637).

References

- Azadifar, M., Paolone, M., Pavanello, D., Rachidi, F., Rakov, V., Romero, C., et al. (2014). An update on the characteristics of positive flashes recorded on the Säntis Tower, paper presented at International Conference on Lightning Protection, Shanghai, China, 11-18 Oct. <https://doi.org/10.1109/ICLP.2014.6973228>
- Azadifar, M., Rachidi, F., Rubinstein, M., Rakov, V. A., Paolone, M., Pavanello, D., & Metz, S. (2016). Fast initial continuous current pulses versus return stroke pulses in tower-initiated lightning. *Journal of Geophysical Research: Atmospheres*, *121*, 6425–6434. <https://doi.org/10.1002/2016JD024900>
- Baba, Y., & Rakov, V. A. (2005). On the use of lumped sources in lightning return stroke models. *Journal of Geophysical Research*, *110*, D03101. <https://doi.org/10.1029/2004JD005202>
- Berger, K. (1967). Novel observations on lightning discharges: Results of research on Mount San Salvatore. *Journal of the Franklin Institute*, *283*(6), 478–525. [https://doi.org/10.1016/0016-0032\(67\)90598-4](https://doi.org/10.1016/0016-0032(67)90598-4)
- Bermudez, J., Rubinstein, M., Rachidi, F., Heidler, F., & Paolone, M. (2003). Determination of reflection coefficients at the top and bottom of elevated strike objects struck by lightning. *Journal of Geophysical Research*, *108*(D14), 4413. <https://doi.org/10.1029/2002JD002973>
- Coles, S., Bawa, J., Trenner, L., & Dorazio, P. (2001). *An introduction to statistical modeling of extreme values* (p. 208). London: Springer-Verlag, Press. <https://doi.org/10.1007/978-1-4471-3675-0>
- Diendorfer, G., Pichler, H., & Mair, M. (2009). Some parameters of negative upward-initiated lightning to the Gaisberg tower (2000–2007). *IEEE Transactions on Electromagnetic Compatibility*, *51*(3), 443–452. <https://doi.org/10.1109/TEMC.2009.2021616>
- Fisher, R., Schnetzer, G., Thottappillil, R., Rakov, V., Uman, M., & Goldberg, J. (1993). Parameters of triggered-lightning flashes in Florida and Alabama. *Journal of Geophysical Research*, *98*(D12), 22,887–22,902. <https://doi.org/10.1029/93JD02293>
- Flache, D., Rakov, V., Heidler, F., Zischank, W., & Thottappillil, R. (2008). Initial-stage pulses in upward lightning: Leader/return stroke versus M-component mode of charge transfer to ground. *Geophysical Research Letters*, *35*, L13812. <https://doi.org/10.1029/2008GL034148>
- He, L., Zhang, Q., Xing, H., & Hou, W. (2014). On validation of FCCFs for lightning striking tall objects considering propagation effect of finitely conducting Earth, 2014 International Conference on Lightning Protection (ICLP) (pp. 1629–1636). Shanghai, China, 11-18 Oct. <https://doi.org/10.1109/ICLP.2014.6973391>
- Heidler, F. H., & Paul, C. (2017). Some return stroke characteristics of negative lightning flashes recorded at the Peissenberg Tower. *IEEE Transactions on Electromagnetic Compatibility*, *59*(5), 1490–1497. <https://doi.org/10.1109/TEMC.2017.2688587>
- Li, D., Azadifar, M., Rachidi, F., Rubinstein, M., Paolone, M., Pavanello, D., et al. (2016). On lightning electromagnetic field propagation along an irregular terrain. *IEEE Transactions on Electromagnetic Compatibility*, *58*(1), 161–171. <https://doi.org/10.1109/TEMC.2015.2483018>
- McEachron, K. (1939). Lightning to the empire state building. *Journal of the Franklin Institute*, *227*(2), 149–217. [https://doi.org/10.1016/S0016-0032\(39\)90397-2](https://doi.org/10.1016/S0016-0032(39)90397-2)
- Miki, M., Rakov, V., Shindo, T., Diendorfer, G., Mair, M., Heidler, F., et al. (2005). Initial stage in lightning initiated from tall objects and in rocket-triggered lightning. *Journal of Geophysical Research*, *110*, D02109. <https://doi.org/10.1029/2003JD004474>
- Mosaddeghi, A., Rachidi, F., Rubinstein, M., Napolitano, F., Pavanello, D., Shostak, V. O., et al. (2011). Radiated fields from lightning strikes to tall structures: Effect of upward-connecting leader and reflections at the return stroke wavefront. *IEEE Transactions on Electromagnetic Compatibility*, *53*(2), 437–445. <https://doi.org/10.1109/TEMC.2010.2076815>
- Pavanello, D., Rachidi, F., Rubinstein, M., Bermudez, J., Janischewskij, W., Shostak, V., et al. (2007). On return stroke currents and remote electromagnetic fields associated with lightning strikes to tall structures: 1. Computational models. *Journal of Geophysical Research*, *112*, D13101. <https://doi.org/10.1029/2006JD007958>
- Pichler, H., Diendorfer, G., & Mair, M. (2010). Some parameters of correlated current and radiated field pulses from lightning to the Gaisberg Tower. *IEEE Transactions on Electrical and Electronic Engineering*, *5*(1), 8–13. <https://doi.org/10.1002/tee.20486>
- Qie, X., Jiang, R., Wang, C., Yang, J., Wang, J., & Liu, D. (2011). Simultaneously measured current, luminosity, and electric field pulses in a rocket-triggered lightning flash. *Journal of Geophysical Research*, *116*, D10102. <https://doi.org/10.1029/2010JD015331>
- Rachidi, F., Janischewskij, W., Hussein, A. M., Nucci, C. A., Guerrieri, S., Kordi, B., & Chang, J.-S. (2001). Current and electromagnetic field associated with lightning-return strokes to tall towers. *IEEE Transactions on Electromagnetic Compatibility*, *43*(3), 356–367. <https://doi.org/10.1109/15.942607>
- Rakov, V. A., Crawford, D. E., Rambo, K. J., Schnetzer, G. H., Uman, M. A., & Thottappillil, R. (2001). M-component mode of charge transfer to ground in lightning discharges. *Journal of Geophysical Research*, *106*(D19), 22,817–22,831. <https://doi.org/10.1029/2000JD000243>
- Rakov, V. A., Thottappillil, R., & Uman, M. A. (1992). Electric field pulses in K and M changes of lightning ground flashes. *Journal of Geophysical Research*, *97*(D9), 9935–9950. <https://doi.org/10.1029/92JD00797>
- Rakov, V. A., Thottappillil, R., Uman, M. A., & Barker, P. P. (1995). Mechanism of the lightning M component. *Journal of Geophysical Research*, *100*(D12), 25,701–25,710. <https://doi.org/10.1029/95JD01924>
- Rakov, V. A., & Uman, M. A. (2003). *Lightning physics and effects* (p. 678). New York: Cambridge University Press. <https://doi.org/10.1017/CBO9781107340886>
- Romero, C., Mediano, A., Rubinstein, A., Rachidi, F., Rubinstein, M., Paolone, M., et al. (2010). Measurement of lightning currents using a combination of Rogowski coils and B-Dot sensors, paper presented at, 30th International Conference on Lightning Protection (ICLP), Cagliari, Italy, 13-17 September. <https://doi.org/10.1109/ICLP.2010.7845959>

- Romero, C., Rachidi, F., Paolone, M., & Rubinstein, M. (2013). Statistical distributions of lightning currents associated with upward negative flashes based on the data collected at the Sántis (EMC) tower in 2010 and 2011. *IEEE Transactions on Power Delivery*, *28*(3), 1804–1812. <https://doi.org/10.1109/TPWRD.2013.2254727>
- Smorgonskiy, A., Rachidi, F., Rubinstein, M., Diendorfer, G., & Schulz, W. (2013). On the proportion of upward flashes to lightning research towers. *Atmospheric Research*, *129-130*, 110–116. <https://doi.org/10.1016/j.atmosres.2012.08.014>
- Thottappillil, R., Goldberg, J. D., Rakov, V. A., Uman, M. A., Fisher, R. J., & Schnetzer, G. H. (1995). Properties of M components from currents measured at triggered lightning channel base. *Journal of Geophysical Research*, *100*(D12), 25,711–25,720. <https://doi.org/10.1029/95JD02734>
- Tran, M., Rakov, V., Ngai, T., Gamarota, W., Pilkey, J., Uman, M., et al. (2013). Microsecond-scale electric field pulses associated with lightning M-components, paper presented at AGU Fall Meeting Abstracts, San Francisco, United States, December, 2013.
- Wang, D., Takagi, N., Watanabe, T., Sakurano, H., & Hashimoto, M. (2008). Observed characteristics of upward leaders that are initiated from a windmill and its lightning protection tower. *Geophysical Research Letters*, *35*, L02803. <https://doi.org/10.1029/2007GL032136>
- Zhang, Q., He, L., Ji, T., & Hou, W. (2014). On the field-to-current conversion factors for lightning strike to tall objects considering the finitely conducting ground. *Journal of Geophysical Research: Atmospheres*, *119*, 8189–8200. <https://doi.org/10.1002/2014JD021496>
- Zhou, H., Diendorfer, G., Thottappillil, R., Pichler, H., & Mair, M. (2011). Mixed mode of charge transfer to ground for initial continuous current pulses in upward lightning, paper presented at 2011 7th Asia-Pacific International Conference on Lightning, Cheng du, China, 1-4 Nov. 2011. <https://doi.org/10.1109/apl.2011.6110212>
- Zhou, H., Diendorfer, G., Thottappillil, R., Pichler, H., & Mair, M. (2012). Measured current and close electric field changes associated with the initiation of upward lightning from a tall tower. *Journal of Geophysical Research*, *117*, D08102. <https://doi.org/10.1029/2011JD017269>
- Zhou, H., Rakov, V. A., Diendorfer, G., Thottappillil, R., Pichler, H., & Mair, M. (2015). A study of different modes of charge transfer to ground in upward lightning. *Journal of Atmospheric and Terrestrial Physics*, *125-126*, 38–49. <https://doi.org/10.1016/j.jastp.2015.02.008>